16th World Conference on Earthquake, 16WCEE 2017
Santiago Chile, January 9th to 13th 2017
Paper N° 920
Registration Code: S-F1463254246

PREDICTION OF DEFORMATION DEMAND ON FRAME BUILDINGS WITH HISTERETIC DAMPERS

J. Oviedo-A[(1)], S. Henao-M[(2)], V. Gómez-M[(3)]

[(1)] *Ph.D., Structural Engineer, F'C Control y Diseño de Estructuras SAS, Medellín, Colombia, joviedo@controldiseno.com*
[(2)] *Structural Engineer, F'C Control y Diseño de Estructuras SAS, Medellín, Colombia, shenao@controldiseno.com*
[(3)] *Civil Engineer, Escuela de Ingeniería de Antioquia, Envigado, Colombia, valengomez@msn.com*
…

Abstract

This study focuses on framed buildings equipped with hysteretic dampers, and introduces a methodology to estimate the seismic deformation demand after damper installation. The proposed methodology considers not only structural and dynamic characteristics of the main frame and dampers, but also input ground motion characteristics. For this purpose, five building structures with 2, 4, 6, 8 and 10 stories were designed according to the Colombian code, and further converted into equivalent single-degree-of-freedom (SDOF) system models. Hysteretic dampers with varying mechanical properties were then installed into the SDOF models. The SDOF models were subjected to a series of 30 input ground motions, which were modified to represent the seismic intensity given in the Colombian code and to grant certain control over the input energy. Nonlinear dynamic analyses were carried out, where parameters such as deformation, acceleration, input energy and hysteretic energy were investigated. The predicted deformation demand obtained from the proposed methodology was compared with that obtained from the analyses. The methodology was shown to be useful for the preliminary assessment of the seismic performance of framed buildings with dampers.

Keywords: hysteretic damper, drift demand, input energy, reinforced concrete frame, earthquake response prediction

1. Introduction

The increasing need to improve safety of building structures against the destructive force of earthquakes has triggered non-traditional seismic protection techniques such as base isolation and energy dissipation systems. These techniques focus on the direct control over the seismic deformation demand to building structures, reducing therefore the structural and non-structural seismic damage.

Although these systems have been successfully applied to building structures worldwide, the application in Colombia has been very limited to a few cases. Two of the main reasons of this situation are: (i) an apparent complexity in the design process (including elaborate analytical models and techniques) together with levels of uncertainty on the performance of the devices, and (ii) the lack of an appropriate amount of time allocated in structural design offices for the analysis and design of buildings that incorporate control techniques [1, 2]. In fact, the later has become a crucial aspect when it comes to propose, to a project owner, the use of a control technique. In general, a project rarely has enough time for appropriate design process. Therefore, it is relevant for design practitioners in Colombia to count on simplified methodologies, particularly at the preliminary stage of the design of a building structure [3].

To date, simplified methodologies such as the use of an equivalent single-degree-of-freedom (SDOF) system, play an important role in the engineering practice as a tool for the seismic evaluation of building structures. Several approaches have been reported in the literature for the use of SDOF models [4-7]. Recently, one of the authors proposed an equivalent SDOF system to represent the behavior of reinforced concrete (R/C) frame buildings equipped with hysteretic dampers [3, 8, 9]. Unlike commonly used SDOF system models, the model proposed by Oviedo *et al.* (2010) [8] takes into account the difference of hysteretic behavior between the R/C main frame and the damper system.

Hysteretic dampers are one of the most prevalent energy dissipating devices used for the seismic protection of building structures. These additional structural elements are incorporated into a main frame structure to dissipate part of the vibration energy imposed by ground motions, reducing therefore the seismic demand on the elements of the main frame. Recently, it has been reported a series of efforts aimed at developing hysteretic dampers in Colombia, as well as introducing and promoting their use in Colombian buildings [10, 11]. These works have certainly gained the attention of the engineering and construction community in Colombia.

Recently, two of the authors studied the behavior of the seismic deformation demand on buildings that incorporate hysteretic dampers. In their work, an analytical procedure for estimating the deformation demand after installing dampers was introduced. The procedure stablishes that the input energy imparted to a frame-damper system is, somehow, proportional to the input energy imparted to the main frame prior to damper installation. In other words, the seismic input energy after damper installation equals the input energy before damper installation multiplied by the factor φ. The factor φ represents the variation of the seismic input energy due to the extent of inelastic response, ground motion characteristics and structural characteristics of the building. Results showed a reasonably good correlation between the deformation demand obtained from nonlinear dynamic analysis and the predicted value.

However, two main limitations were reported in the study. The first one has to do with the lack of a theoretical expression completely independent of the results of dynamic analysis. The second one has to do with a significant variation in the energy input among the ground motions used for that work; which was mainly because all source records were modified to match the acceleration design spectrum. Therefore, the present study extends this previous work by including (i) a better control over the seismic input energy and deformation demand, (ii) a larger series of ground acceleration records for nonlinear analysis, (iii) an evaluation of the definition of the factor φ, and (iv) a practical expression for estimating the seismic deformation demand after installing dampers to an R/C main frame.

For this purpose, five R/C frame buildings with 2, 4, 6, 8 and 10 stories were studied as representative of low- to mid-rise building structures. Buildings were designed according to the Colombian seismic code (NSR-10), and further converted into equivalent SDOF systems according to the methodology proposed by Kuramoto *et al.* (2000) [7]. Hysteretic dampers with different mechanical properties were installed into the equivalent SDOF models, and a series of nonlinear dynamic analyses were performed both on the SDOF systems of the building without dampers as well as on the buildings after damper installation. A total of 30 input ground motions were selected and modified to represent the seismic intensity given the Colombian code, and to grant control over the seismic input energy and deformation demand on the systems. This aspect is very important for getting adequate and comparable response quantities. After performing the analyses, the behavior of deformation demand and the definition of the factor φ was investigated, and a methodology for predicting the seismic deformation demand was then proposed.

2. Building Model

2.1 R/C main frame

The five three-dimension moment-resistant, strong-column and weak-beam R/C main frames considered in this study are shown in Fig.1. The vertical load (dead + live) per unit area is assumed to be the same for all stories with a typical floor load of 9.61 kN/m^2. The vertical load for the roof, however, was set to 7.75 kN/m^2. Prior to damper installation, the structural design of all five buildings was established based on the current Colombian seismic code NSR-10 [12]. Details of the structural design and design parameters of the studied buildings can be found in [10]. Table 1 summarizes the structural and dynamic characteristics of the R/C main frames.

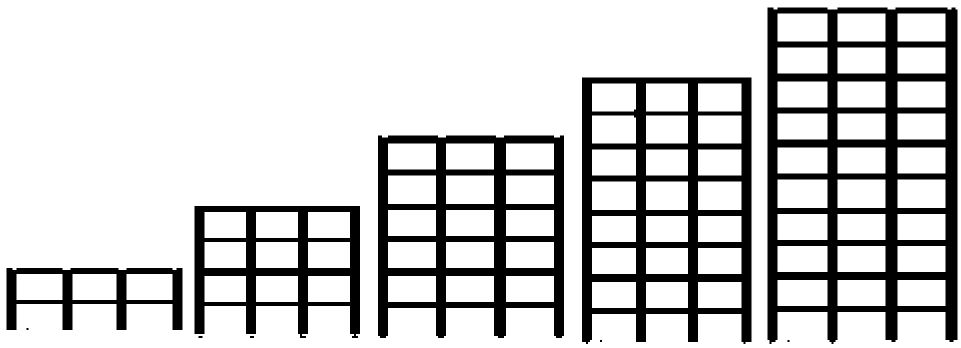

Fig. 1 – Elevation of the studied R/C main frames

Table 1 – Structural properties of R/C main frames

# Stories	Total height	Period	Weight	Beams		Columns	
				Cross section	Concrete Strength	Cross Section	Concrete Strength
	(m)	(seg)	(kN)	(cm)	MPa	(cm)	MPa
2	6.60	0.44	4085	30x35	21	40x40	21
4	13.20	0.73	9720	40x40	21	45x45	28
6	19.80	0.87	16458	40x45	21	60x60	28
8	26.40	1.03	23977	40x50	21	70x70	28
10	33.00	1.19	36464	40x50	21	100x100	28

2.2 Conversion of the R/C main frame into an equivalent SDOF system

The five buildings described in the previous section are converted into equivalent SDOF systems models according the methodology proposed by Kuramoto [7]. Table 2 summarizes the structural and dynamic characteristics of the five SDOF models. These five models are later used for nonlinear dynamic analyses to serve as a reference point for comparison with the response of the buildings with dampers.

Table 2 – Structural properties of the SDOF systems for the R/C main frames

# Stories	W (kN)	Period T (s)	Q_{Fc} (kN)	Δ_{Fc} (cm)	Q_{Fy} (kN)	Δ_{Fy} (cm)
2	3532	0.41	263	0.31	967	2.26
4	7984	0.70	529	0.81	1645	5.37
6	13048	0.78	665	0.77	2608	7.18
8	18680	0.84	891	0.83	3633	8.11
10	26788	0.97	991	0.86	4371	8.47

2.3 Damper system

Hysteretic dampers are then incorporated into the SDOF system models that represent the R/C main frames. The restoring force characteristics of the entire system (R/C main frame + dampers) is then idealized as the combination of two springs connected in parallel, as shown in Fig.2. Here, Q_S, Q_{Fy} and Q_{Dy} are the yield shear strength of the entire system, R/C main frame and damper system, respectively. Δ_{Fc}, Δ_{Fy}, Δ_{Dy}, Δ_{max}, μ_F, μ_D are the cracking story drift, the yield story drift of the R/C main frame, the yield story drift of the damper system, the maximum story drift, the ductility of the R/C main frame and the ductility of the damper system, respectively. α and ρ define the shear at the cracking point Q_{Fc} and the equivalent stiffness K_{eq} for the R/C main frame, respectively.

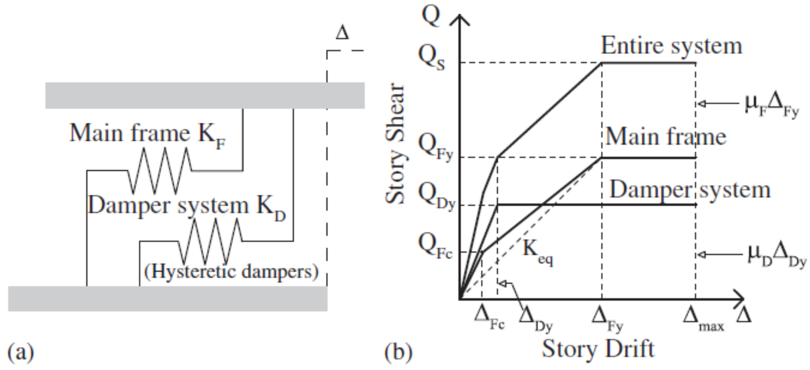

Fig. 3 – SDOF system model for an R/C main frame with a damper system: (a) schematic configuration and (b) restoring force characteristics (taken from [7])

The structural characteristics of the damper system, i.e., yield strength and stiffness, are assumed to be proportional to those of the R/C main frame. To determine the yield strength Q_{Dy} and the stiffness K_D of the damper system, the damper strength ratio β (hereafter the strength ratio) and the damper yield drift ratio ν (hereafter the drift ratio) are used. Thus, referring to Fig.3, Q_{Dy}, Q_{FY}, Δ_{FY} and Δ_{DY} are related by:

$$Q_S = Q_{Fy} + Q_{Dy} \tag{1}$$

$$Q_{Dy} = \beta Q_{Fy} \tag{2}$$

$$\Delta_{Dy} = \nu \Delta_{Fy} \tag{3}$$

To define the restoring force characteristics of the SDOF model for an entire system, the value of ν was varied from 0.1 to 1.0 with an interval of 0.1, and the value of β varied from 0.1 to 0.9 with an interval of 0.1. Finally, the elastic stiffness of the dampers system K_D is determined by:

$$K_D = {Q_{Dy}}/{\Delta_{Dy}} \tag{4}$$

With damper installation, the total stiffness and strength of the entire system are increased, and the dynamic properties are then modified. Eq. (5) represents the value of the natural period of the entire system T as a function of β, ρ, ν, and the natural period of the R/C main frame T_0. Fig.4 shows the variation of the natural period T of analyzed models after installing hysteretic dampers, and Fig. 5 shows the variation of the stiffness of the entire system K_S. In general, it can be seen that the natural period shortens with increasing values of β and decreasing values of ν.

$$T = T_0\sqrt{\frac{1}{1+\rho\frac{\beta}{\upsilon}}} \tag{5}$$

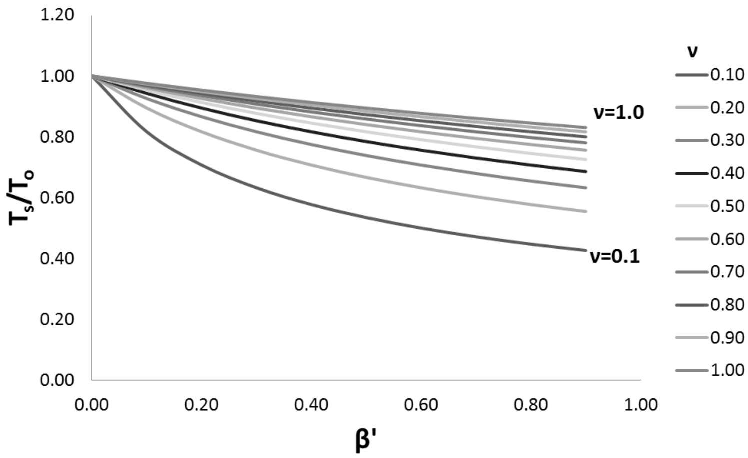

Fig. 4 – Variation of natural period of analyzed SDOF models with respect to β and ν

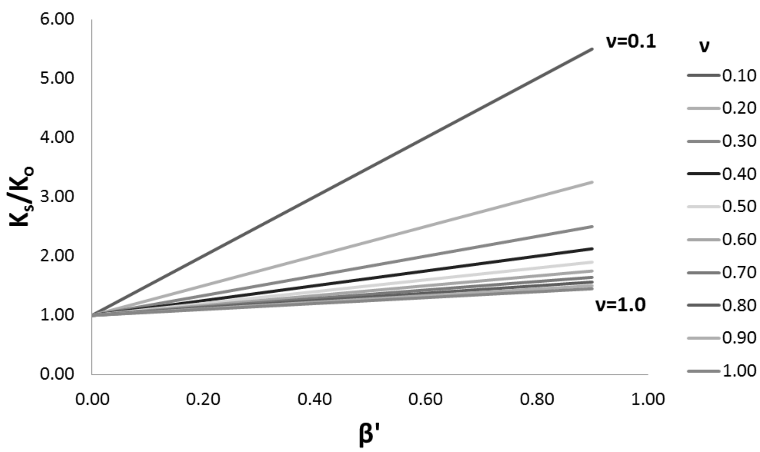

Fig. 5 – Variation of total stiffness of analyzed SDOF models with respect to β and ν

3. Earthquake Response Analysis

3.1 Input ground motions

The input ground motions used for the nonlinear time-history analyses are summarized in Table 3. All source records represent near-fault type earthquakes, categorized within a type C soil (dense soils or soft rock - $360\,m/s \leq \mathrm{Vs}_{30} \leq 760\,m/s$, where Vs_{30} is the average shear wave velocity down to a depth of 30 m) according to NSR-10. Thus, all records have an epicentral distance of no more than 20 km, and present single velocity pulses of significant amplitude. All acceleration records were obtained from the Pacific Earthquake Engineering Research Center (PEER) website. In Table 3, the Arias Intensity is also shown [13].

As mentioned earlier, unlike the previous work done by two of the authors, this study considers a better control over the input energy imparted to the buildings. This is achieved by modifying the source records so that the response spectrum of a source record matches the design velocity spectrum given in the Colombian code. The use of a design velocity spectrum instead of the design acceleration spectrum, leads to a relative uniform energy input among all modified records. Fig.6 shows the velocity spectra and the energy spectra as an equivalent velocity V_{eq}. It can be seen a relative small variation of the input energy. These 30 modified records are then grouped into Case I records.

Table 3 – Source input ground motions

					Original Record			Modified Record, Case II		
ID	Event	Year	Station	Magnitude	PGA (cm/s2)	PGV (cm/s)	IA (cm/s)	PGA (cm/s2)	PGV (cm/s)	IA (cm/s)
33-1	Parkfield	1966	Temblor pre-1969	6.19	352	21	45	232	41	103
33-2	Parkfield	1966	Temblor pre-1969	6.19	264	15	31	268	39	143
50-1	Lytle Creek	1970	Wrightwood - 6074 Park Dr	5.33	158	10	13	382	49	102
50-2	Lytle Creek	1970	Wrightwood - 6074 Park Dr	5.33	197	10	15	232	59	132
71-1	San Fernando	1971	Lake Hughes #12	6.61	356	15	93	270	49	107
71-2	San Fernando	1971	Lake Hughes #12	6.61	278	12	78	295	39	108
106-1	Oroville-01	1975	Oroville Seismograph Station	5.89	90	4	4	284	60	99
107-1	Oroville-02	1975	Oroville Airport	4.79	36	3	0	210	71	111
107-2	Oroville-02	1975	Oroville Airport	4.79	15	2	0	262	50	95
109-1	Oroville-04	1975	Medical Center	4.37	77	3	1	291	59	90
109-2	Oroville-04	1975	Medical Center	4.37	43	2	1	268	65	93
110-1	Oroville-04	1975	Oroville Airport	4.37	20	2	0	272	62	95
110-2	Oroville-04	1975	Oroville Airport	4.37	23	1	0	298	33	89
113-1	Oroville-03	1975	DWR Garage	4.7	138	1	3	295	56	98
113-2	Oroville-03	1975	DWR Garage	4.7	206	2	13	330	68	101
114-1	Oroville-03	1975	Duffy Residence (OR5)	4.7	83	2	2	309	65	88
114-2	Oroville-03	1975	Duffy Residence (OR5)	4.7	60	2	2	308	68	94
115-1	Oroville-03	1975	Johnson Ranch	4.7	188	4	13	404	62	105
115-2	Oroville-03	1975	Johnson Ranch	4.7	94	2	5	245	58	113
116-2	Oroville-03	1975	Nelson Ranch (OR7)	4.7	112	2	3	261	61	103
117-2	Oroville-03	1975	Oroville Airport	4.7	45	1	1	247	55	106
120-2	Oroville-03	1975	Up & Down Cafe (OR1)	4.7	149	4	5	315	59	96
125-1	Friuli-Italy-01	1976	Tolmezzo	6.5	345	22	78	239	82	105
125-2	Friuli-Italy-01	1976	Tolmezzo	6.5	309	31	120	232	44	102
132-1	Friuli-Italy-02	1976	Forgaria Cornino	5.91	254	9	29	206	55	106
132-2	Friuli-Italy-02	1976	Forgaria Cornino	5.91	208	10	37	178	48	102
145-1	Coyote Lake	1979	Coyote Lake Dam (SW Abut)	5.74	155	11	19	251	39	110
145-2	Coyote Lake	1979	Coyote Lake Dam (SW Abut)	5.74	274	20	36	306	75	120
150-1	Coyote Lake	1979	Gilroy Array #6	5.74	427	49	77	391	81	114
150-2	Coyote Lake	1979	Gilroy Array #6	5.74	310	25	68	356	63	96

Another group of modified records was also studied. Case II ground motions include 30 records modified to match a design energy spectrum. Since the Colombian code does not consider this design spectrum, a design energy spectrum was then obtained through the velocity design spectrum of the Colombian code. More details on the assumed design energy spectrum can be found in [14]. Fig.7 shows the velocity and energy spectra of the Case II records (dashed line indicates the target design spectrum). It is clear after comparing Case I and Case II response spectra that Case II records grant less variation of the input energy, and therefore, a more uniform deformation demand can be expected among all 30 records. Consequently, the Case II records were used for the nonlinear dynamic analyses. Table 3 also lists some characteristics of the modified records of the Case II motions.

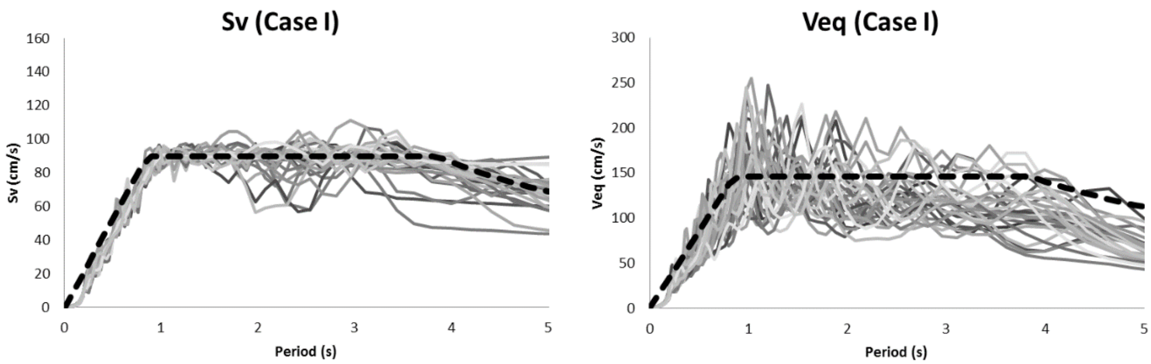

Fig. 6 – Response spectra of Case I records. Left: velocity spectra. Right: energy spectra

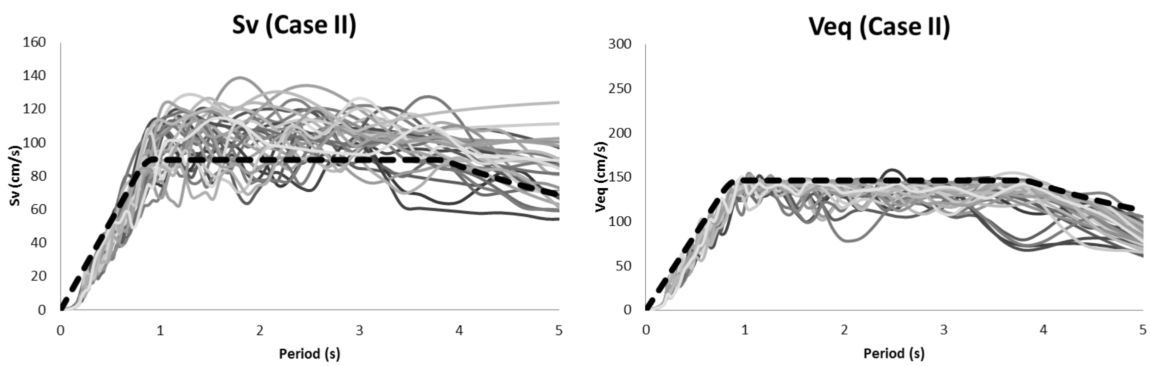

Fig. 7 – Response spectra of Case II records. Left: velocity spectra. Right: energy spectra

3.2 Nonlinear dynamic analysis

In the numerical analyses of the SDOF systems, a 2-spring SDOF model with the degrading trilinear Takeda model to represent the hysteretic behavior of the R/C main frame and with a bilinear model to represent dampers was used. Damping ratio of 3% of the critical, integration time step of 0.005 s, and a post-elastic stiffness ratio of 0.01 was assumed in all analyses. The series of analyses correspond to the following cases: (1) five numbers of stories (n= 2, 4, 6, 8, 10), (2) nine strength ratios (β= 0.1 to 0.9), (3) ten drift ratios (ν= 0.1 to 1.0), and (4) the 30 modified input ground motions listed in Table 3. In total more than 27,300 analyses were performed.

4. Prediction of Deformation Demand

According to previous studies [10, 14], the prediction of the seismic deformation demand after installing dampers to an R/C building structure is based on the premise that the input energy imparted to the entire system (R/C main frame + dampers) equals the input energy imparted to the R/C main frame multiplied by a factor φ (see Eq. (6)) The factor φ represents the variation in the seismic input energy with damper installation. As shown in previous works [10], the input energy might vary due to the change of strength, stiffness and natural period after damper installation, as well as to the extent of inelastic response and ground motion characteristics.

$$\mathrm{E_{i0}} = \varphi \mathrm{E_i} \tag{6}$$

Where, E_i and E_{i0} stand for the input energy of the entire system and the input energy of the R/C main frame, respectively. Then, assuming that the total input energy is dissipated only by the hysteretic energy work, Eq. (6) can be rewritten as in Eq. (7). Here, E_{HF}, E_{HF0} and E_{HD} stand for the hysteretic energy of the R/C main frame after damper installation, hysteretic energy of the R/C main frame before dampers, and hysteretic energy of the damper system.

$$E_{HF0} = \varphi(E_{HF} + E_{HD}) \tag{7}$$

Moreover, this hysteretic energy can be obtained from the work of the entire system under monotonically increasing loads, as shown in Fig.8. In other words, the hysteretic energy is obtained through the area under the force-deformation curve. Here, it is important to note that the relationship depicted in Fig.8 is only a reasonable approximation of the comparative behavior of the energy absorbed by the interaction of the two systems (R/C main frame and dampers). Thus, since no time-depending response factors can be considered, the use of the factor φ is needed. In Fig.8, Δ_{max} and Δ'_{max} stands for the maximum deformation of the R/C main frame and the maximum deformation of the entire system after damper installation, respectively.

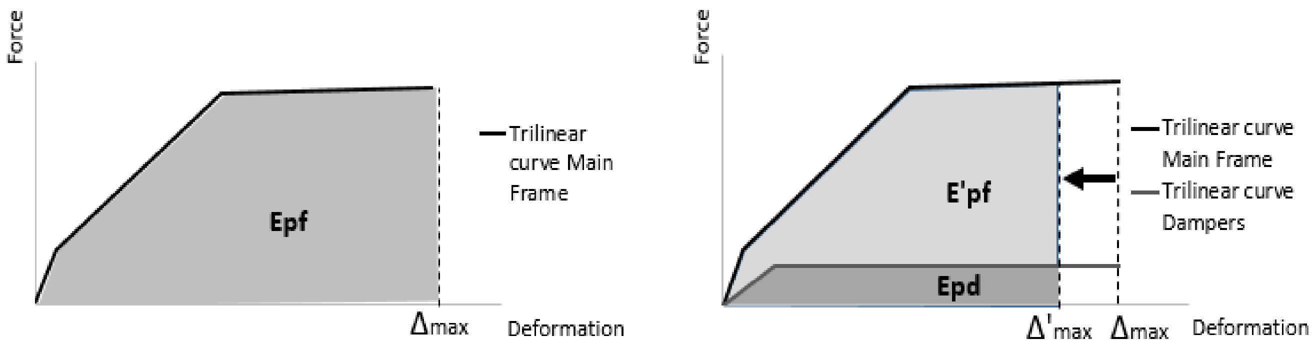

Fig. 8 – Force-deformation monotonic curve: (a) without dampers and (b) with dampers

From Fig.8 two cases apply: Case (1) applies when both the R/C main frame and the damper system behave inelastically ($\Delta'_{max} > \Delta_{Fy}$ and $\Delta'_{max} > \Delta_{Dy}$), and Case (2) applies when only the damper system is in the inelastic range ($\Delta'_{max} > \Delta_{Dy}$). Therefore, Eq. (7) can be rewritten, depending on the previous cases, as:

For Case (1)

$$\frac{\Delta' max}{\Delta\, max} = \frac{1}{\varphi(1+\beta)} + \frac{\nu\,\beta}{2\,\mu_{F0}\,(1+\beta)} + \frac{(1-\varphi)(\alpha-\alpha\rho-1)}{2\,\mu_{F0}\,\varphi\,(1+\beta)} \tag{8.1}$$

For Case (2)

$$A\left(\frac{\Delta' max}{\Delta max}\right)^2 + B\left(\frac{\Delta' max}{\Delta max}\right) + C = 0 \tag{8.2}$$

where,

$$A = \varphi\frac{1-\alpha}{1-\alpha\rho}\mu_{F0} \tag{8.2.1}$$

$$B = \varphi\left(1 - \frac{1-\alpha}{1-\alpha\rho} + \alpha - \alpha\rho\frac{1-\alpha}{1-\alpha\rho} + 2\beta\right) \tag{8.2.2}$$

$$C = \frac{1}{\mu_{F0}}\left(\alpha\rho\left(\varphi\frac{1-\alpha}{1-\alpha\rho} - \varphi + 1\right) - 2\mu_{F0} - \alpha - \varphi\nu\beta + 1\right) \tag{8.2.3}$$

Thus, the series of equations above presented are used for the prediction of the maximum deformation demand Δ'_{max} after installing dampers to an R/C main frame. It is important to note that a reasonable estimate of the response of the R/C main frame subjected to a ground motion prior to damper installation is needed for predicting Δ'_{max}. In practical terms, one can predict a possible reduction in the deformation demand once dampers are installed with certain mechanical characteristics, depending on the values of β and ν. However, as suggested by the series of Eqs. (8), the value of the factor φ is still needed.

4.1 Evaluation of the factor φ

As previously mentioned, the value of factor φ is needed for the prediction of Δ'_{max}, and depends on structural, dynamic and ground motions parameters. To solve this issue, the behavior of the factor φ was investigated through both the variation of the input energy and the variation of the hysteretic energy. The top row of Fig.9 depicts the relationship between the exact value of φ (hereafter φ_{real}) obtained from the results of the nonlinear analyses through Eq. (6) and the value of φ required to satisfy the series of Eqs. (8) (hereafter φ_{req}). On the other hand, the bottom row of Fig.9 depicts the relationship between φ_{real} obtained through Eq. (7) and the value of φ_{req}. The value of φ_{req} can be readily calculated now that both Δ_{max} and Δ'_{max} are known from the analyses. Fig.9 clearly indicates that it is rather complicated to stablish an adequate correlation between both factors, no matter the definition used for determining the value of φ.

Another aspect to consider is the evaluation of φ_{real}. At the preliminary stage of a structural design of a building structure equipped with dampers, it is not possible to determine the value of φ_{real} unless several nonlinear analyses are performed. Therefore, a theoretical value for φ_{real} (hereafter φ_{theo}) and a correlation between the two factors is needed. Gómez [14] studied different expressions for input energy evaluation proposed in the literature, and showed that the equation proposed by Housner [15] led to a better correlation, compared to other definitions. Further details can be found in [14]. On the other hand, a theoretical value for φ_{real} seems not available through hysteretic energy variation, as in Eq. (7).

4.2 Simplified prediction

From the results of the previous section, it was concluded that a proper expression for the factor φ is somehow complicated to achieve. It was also concluded that determining the value of φ from the input energy or hysteretic energy has a major issue: there is a significant difference between the behavior of both input and hysteretic energy and the behavior depicted in Fig.8 due to nature of loading. Moreover, both cases lack a proper theoretical value which one can use in the preliminary stage of a structural design. Thus, after identifying other directions for solving the issue of the factor φ, a simplified prediction is then presented.

Eq. (7) can be rewritten as in Eq. (9) by using the areas under the force-deformation curve in Fig. 8. Here, A_F, A_{F0} and A_D stand for the absorbed energy by the R/C main frame after damper installation, absorbed energy by the R/C main frame before dampers, and the absorbed energy by the damper system.

$$\mathrm{A_{F0}} = \mathrm{A_F} + \mathrm{A_D} \tag{9}$$

Fig.10 shows the relationship between Δ'_{max} / Δ_{max} and T / T_0 for the series of ground motions of Table 4. The data shown in Fig.10 correspond to average values among all ground motions. It can be seen that there is a tendency of decreasing Δ'_{max} / Δ_{max} with the decrease of T / T_0. Thus, the result obtained through either the Eq. (8.1) or (8.2), with the value of φ set to unity, is then affected according to Eq. (10) to serve as a correction factor. This is:

$$\frac{\Delta'\max}{\Delta\max} = \left(\frac{T}{T_0}\right)\left(\frac{\Delta'\max}{\Delta\max}\right)_{Eq.(8)} \tag{10}$$

It is worth noting that a reasonable estimate of the response of the R/C main frame subjected to a ground motion prior to damper installation is needed for predicting Δ'_{max}. In other words, a reasonable estimate of μ_{F0} is needed. To solve this issue, and based on the well-known equal displacement rule, the value of μ_{F0} in Eqs. (8) can be approximated using a design spectrum (S_d or S_a) as:

$$\mu_{F0} \approx \frac{Sd_{(T=T_0)}}{\Delta_{Fy}} = \frac{(T_0)^2 Sa_{(T=T_0)}}{4\pi^2 \Delta_{Fy}} \tag{11}$$

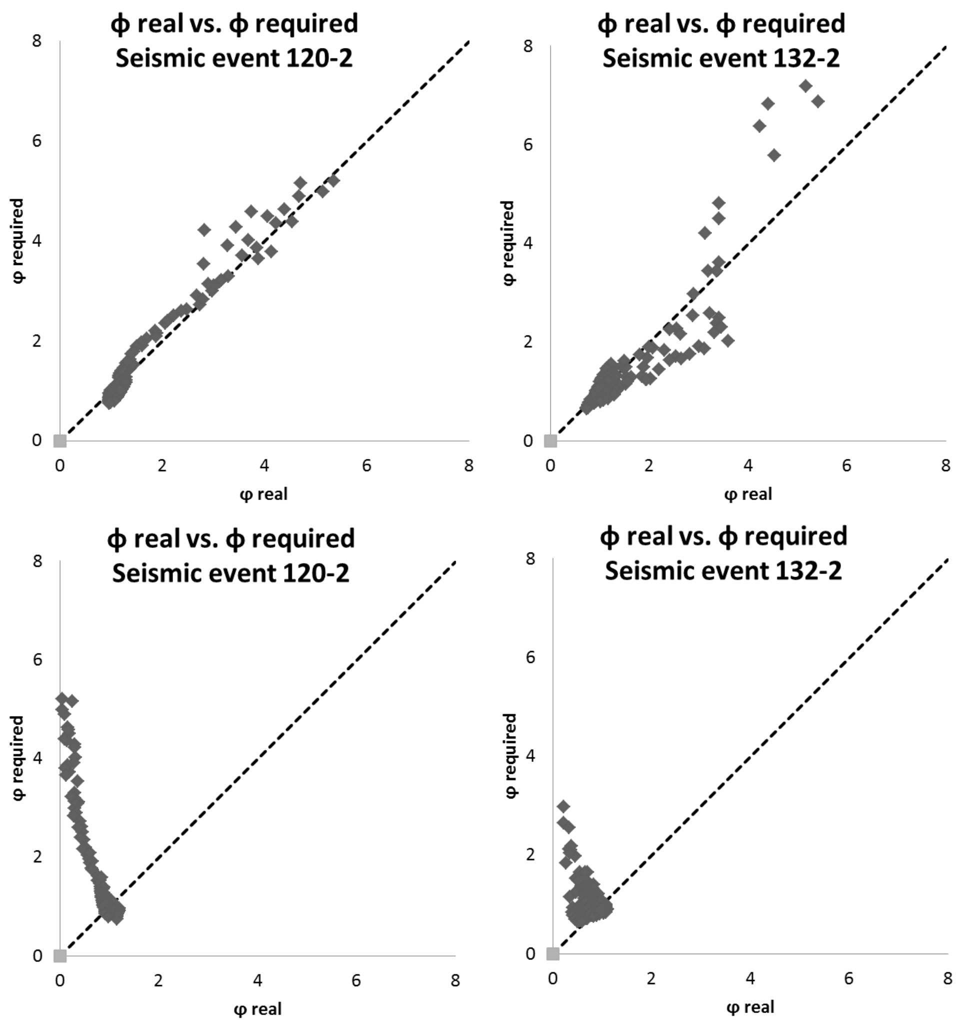

Fig. 9 – Relationship between φ_{real} and φ_{req}. Top row: value of φ_{real} obtained through Eq.(6). Bottom row: value of φ_{real} obtained through Eq.(7)

Fig.11 shows the correlation between the exact value of Δ'_{max} / Δ_{max} obtained from the nonlinear analyses and the predicted value obtained from Eqs. (8) and (10) (dashed line indicates ±20%); here, the value of μ_{F0} was determined using the Eq. (11). Values shown in Fig.11 correspond to analysis cases with $\beta \leq 0.5$ and $\nu \leq 1.0$ according to previous studies which show that dampers are more effective within this range [3, 10, 16]. It can be clearly observed that the simplified methodology leads to predictions that can be used in the design practice for the case of SDOF systems.

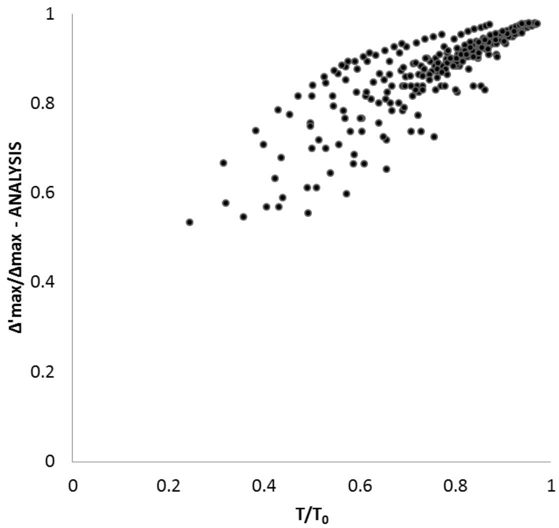

Fig. 10 – Relationship between Δ'_{max} / Δ_{max} and T / T_0

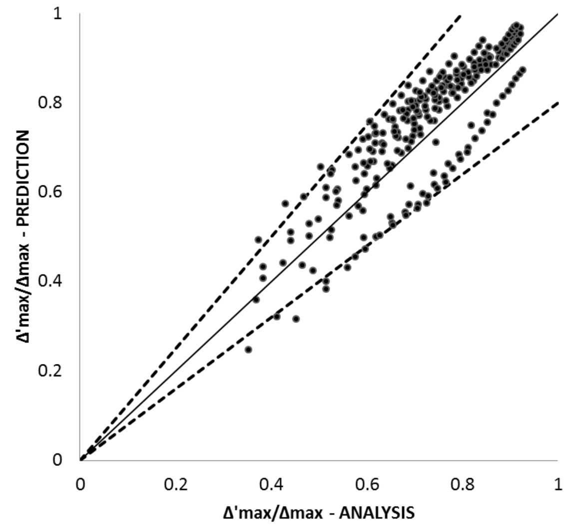

Fig. 11 – Prediction of Δ'_{max} / Δ_{max}

It is worth noting that this methodology has been proven useful for the case of an equivalent SDOF system that represents the behavior of a whole R/C building equipped with dampers. On the other hand, with regards to estimating the story drift demand on MDOF systems, the authors are working on this issue through the series of Eqs. (8) and the methodology proposed by Oviedo *et al.* (2010, 2011) [3, 8].

5. Conclusions

The behavior of deformation demand on R/C frame buildings with hysteretic dampers was investigated and a methodology for predicting the seismic deformation demand was presented. Based on the results of nonlinear dynamic analyses on equivalent SDOF systems, it is concluded that the proposed methodology for predicting the seismic deformation demand after installing dampers into an R/C main frame leads to adequate estimates that can be used by design practitioners at the preliminary design stage. With this estimate, the designer can then set the mechanical properties of dampers required to achieve a desired structural performance. Finally, the methodology herein proposed is expected to contribute to ongoing efforts for the seismic response control of building structures with hysteretic dampers, and to encourage the use of hysteretic dampers in Colombia.

6. References

[1] Oviedo-Amezquita JA, Uribe P (2006): Seismic response control systems in building structures. *Revista EIA*, **6**, 105-120.

[2] Oviedo-Amezquita JA, Uribe P (2009): Metallic hysteretic dampers as a seismic response control technique in Colombian buildings. *Revista EIA*, **11**, 51-63.

[3] Oviedo-A JA, Midorikawa M, Asari T (2011): An equivalent SDOF system model for estimating the response of R/C building structures with proportional hysteretic dampers subjected to ground motions. *Earthquake Engineering & Structural Dynamics*, **40**, 571-489.

[4] Freeman SA, Nicoletti JP, Tyrell JV (1975): Evaluation of existing buildings for seismic risk – A case study of Puget Sound Naval Shipyard, Bremerton, Washington. *Proceedings of the 1st U.S National Conference on Earthquake Engineering*, Washington, USA.

[5] ATC-40 (1996): Seismic evaluation and retrofit of concrete structures. Products 1.2 and 1.3 of the Preposition 122 seismic retrofit practices improvement program, California Safety Commission. *Report No. SSC 96-01, ATC-40*, Applied Technology Council, California, USA.

[6] FEMA-273 (1997): *HEHRP Guidelines for the Seismic Rehabilitation of Buildings*, Federal Emergency Management Agency, Washington, USA.

[7] Kuramoto H, Teshigawara M, Okuzono T, Koshika N, Takayama M, Hori T (2000): Predicting the earthquake response of buildings using equivalent single degree of freedom system. *Proceedings of the 12th World Conference on Earthquake Engineering*, Auckland, New Zealand.

[8] Oviedo-A JA, Midorikawa M, Asari T (2010): An equivalent SDOF system model for estimating the earthquake response of R/C buildings with hysteretic dampers. *Proceedings of the 14th European Conference on Earthquake Engineering*, Ohrid, Macedon.

[9] Oviedo JA, Londoño CC (2013): Modelo inelástico simplificado para la predicción de la respuesta sísmica de pórticos en concreto con disipadores de energía. *VI Congreso Nacional de Ingeniería Sísmi*ca, Medellín, Colombia.

[10] Henao S, Garza L, Oviedo JA (2013): Demanda de deformación en edificaciones con y sin disipadores de energía. *VI Congreso Nacional de Ingeniería Sísmica*, Medellín, Colombia.

[11] Oviedo JA, Buitrago JJ, Patiño JC, Hoyos D (2015): Evaluación experimental del desempeño de un disipador de energía por deformación tipo riostra. *VII Congreso Nacional de Ingeniería Sísmica*, Bogotá, Colombia.

[12] NSR-10 (2010): *Reglamento Colombiano de Construcciones Sismo resistentes*, Asociación Colombiana de Ingeniería Sísmica, Bogotá, Colombia.

[13] Arias A (1970): *A measure of earthquake intensity. Seismic design for nuclear power plants*, Hansen RJ (Ed.), MIT Press, Cambridge.

[14] Gómez V (2015): Seismic Deformation Demand in RC Frame Buildings with and without Energy Dampers. Civil Engineering Graduation *Report*, Escuela de Ingeniería de Antioquia, Envigado, Colombia.

[15] Housner GW (1959): Behavior of structures during earthquakes. *Journal of the Engineering Mechanics Division*, **85**(4), 109-129.

[16] Oviedo-A JA, Midorikawa M, Asari T (2010): Earthquake response of ten-story story-drift-controlled reinforced concrete frames with hysteretic dampers. *Engineering Structures*; **32**(6), 1735–1746.